Available online at www.sciencedirect.com
ScienceDirect
Journal of the European Ceramic Society 27 (2007) 1237–1245
www.elsevier.com/locate/jeurceramsoc

The influence of post-sintering HIP on the microstructure, hardness, and indentation fracture toughness of polymer-derived Al_2O_3–SiC nanocomposites

Dušan Galusek [a,b,*], Jaroslav Sedláček [a], Peter Švančárek [a], Ralf Riedel [b], Raphaelle Satet [c], Michael Hoffmann [c]

[a] *Vitrum Laugaricio – Joint Glass Center of the Institute of Inorganic Chemistry, Slovak Academy of Sciences, Alexander Dubček University of Trenčín, and RONA, j.s.c., Študentská 2, 911 50 Trenčín, Slovak Republic*
[b] *Institute of Materials Science, Darmstadt University of Technology, Petersenstrasse 23, D-64287 Darmstadt, Germany*
[c] *Institut für Keramik in Maschinenbau, University of Karlsruhe, Haid-und-Neu-Str. 7, D-76131 Karlsruhe, Germany*

Available online 12 May 2006

Abstract

Al_2O_3–SiC nanocomposites containing 3–8 vol.% SiC were prepared from fine α-alumina powder and a poly(allyl)carbosilane precursor of SiC by polymer infiltration of porous alumina matrix (composites IP), or by warm pressing of polymer-coated alumina powder (composites CW). The polymer was converted to SiC by careful heating of green specimens in inert atmosphere (Ar). The residual porosity was eliminated to less than 10% by pressureless sintering (PS) at temperatures between 1700 and 1850 °C. The post-sintering hot isostatic pressing (HIP) at 1700 °C eliminated the residual porosity to less than 1%, but also resulted in coarsening of the alumina matrix grains, and the inter- and intragranular SiC inclusions. The Vickers hardness of IP specimens sintered at $T < 1850$ °C increased by 1–10%, which is attributed to elimination of residual porosity. The hardness and indentation fracture toughness of specimens IP sintered at 1850 °C decreased after HIP by 6 and 15%, respectively. The HIP of CW composites increased their hardness and fracture toughness by approximately 10%. The maximum fracture toughness of 5.2 ± 0.2 MPa $m^{1/2}$ was measured for the materials containing 8 vol.% of SiC. A correlation was found between the fracture toughness, and the mean size and volume fraction of intergranular SiC inclusions in composites CW.

Keywords: Hot isostatic pressing; Precursors-organic; Microstructure-final; Mechanical properties; Al_2O_3–SiC

1. Introduction

Nearly two decades after Niihara reported extraordinary strength of nanocomposites[1] many questions remain unanswered. Not only that the mechanism of strengthening is not clear, and various works suggest different mechanisms,[1–7] but many authors failed to reproduce the data of Niihara entirely, and report various levels of strengthening.[7–10]

Even though the increase of fracture toughness in nanocomposites was never reported to be high, the results achieved by various authors are still more controversial. While several papers reported modest increase of toughness of nanocomposites over that of unreinforced ceramics,[11] others did not find any appreciable change,[7,9,10] or even reported a reduction in the fracture toughness depending on the measurement technique.[7] One possible reason for these uncertainties may be the fact that the mechanical properties of nanocomposites are strongly influenced by slight changes of the processing route.[12] Another factor, whose role is not clear, is the role of intra- and intergranular SiC particles in determining the mechanical properties, especially fracture toughness. In contrast to pure monolithic alumina, which fails usually by grain boundary fracture, cracks in Al_2O_3–SiC nanocomposites follow almost entirely transgranular path. Some authors suggest that the change of the fracture mode is caused by tensile tangential stresses in alumina matrix grains around intragranular SiC inclusions. Combined with radial, grain boundary strengthening compressive stresses, these stresses deflect cracks into alumina matrix grains so that they follow transgranular path, being attracted by intragranular SiC inclusions. The increase of fracture energy is not observed,

* Corresponding author. Tel.: +421 32 7400262; fax: +421 32 7400251.
E-mail address: galusek@tnuni.sk (D. Galusek).

0955-2219/$ – see front matter © 2006 Elsevier Ltd. All rights reserved.
doi:10.1016/j.jeurceramsoc.2006.04.028

as the increase of toughness resulting from the change of fracture mode from intergranular to transgranular is compensated by the fact that the crack passes through tensile stress fields between second phase and matrix particles.[9] However, Jiao and Jenkins who performed a detailed analysis of crack propagation in nanocomposites observed no such attraction, even in a crack moving very close to an intragranular SiC particle.[13] Other authors consider the ratio of volume fractions of intra- and intergranular SiC as an important parameter, which influences the fracture toughness of nanocomposites. The cracks are attracted to intergranular particles due to the formation of tensile residual stress fields around particles, and perpendicular to adjacent boundaries. This mechanism is expected to increase crack deflection length, at least to certain extent, and thus to contribute to toughening of the nanocomposite.[11]

Our previous works report in detail on the preparation of alumina-silicon carbide nanocomposites by free sintering, and with the use of a poly(allyl)carbosilane precursor as the source of SiC.[14,15] The volume fraction, and to certain extent also the size, and location of SiC particles in alumina matrix can be controlled by adjusting the concentration of the polymer, and by the fraction and size of open pores in infiltrated alumina matrix. The resulting ceramics consist of relatively fine-grained alumina grains (the mean grain size $\geq$1 μm, depending on the volume fraction of SiC and conditions of sintering). The ratio of volume fractions of inter- and intragranular SiC particles was found to vary systematically with the volume fraction of SiC and with the temperature of sintering.[16] Hardness and indentation fracture toughness of free sintered specimens were higher than those usually reported for monolithic alumina, but the improvement was not significant and the values are comparable to the values reported for the nanocomposites Al_2O_3–SiC in the literature.[17]

This work reports on of the influence of post-sintering HIP on microstructure development, hardness, and indentation fracture toughness of free sintered Al_2O_3–SiC nanocomposites.

2. Experimental

The Al_2O_3–SiC nanocomposites were prepared from the α-alumina powder Taimicron TM DAR (Taimei Chemicals Co., Ltd., Japan) and an organosilicon polymeric SiC precursor (poly(allyl)carbosilane SP-M, StarFire Systems, Watervliet, NY). Two processing routes were investigated: (a) infiltration of the pre-sintered alumina matrix with a solution of the polymer (samples IP), and (b) coating of the alumina powder with a solution of the polymer (samples CW), followed by axial pressing of coated powder at elevated temperature (warm pressing).

2.1. Infiltration

Approximately 1 g of the alumina powder was pressed axially in a steel die at 50 MPa and then isostatically at 500 MPa in order to prepare pellets with the diameter of 12 mm and of 6 mm height. The alumina green bodies were then pre-sintered in air in an electrical furnace at 1160 °C without isothermal dwell in order to ensure sufficient handling strength, and to maintain the open porosity at desirable level.

The pre-sintered alumina pellets were then infiltrated with the concentrated liquid polymer (specimens containing 8 vol.% SiC and denoted as IP8), or by the solution of the polymer in water-free cyclohexane (specimens containing 3, or 5 vol.% SiC and in the following text denoted as IP3, or IP5, respectively). The concentration of the polymer in the solution was adjusted so as to achieve the required volume fraction of SiC in the composite. The infiltration was carried out in protective Ar atmosphere at decreased pressure (approximately 50 Pa) in order to facilitate penetration of the polymer into the alumina matrix, and to avoid extended exposure of the polymer to moisture and air. After infiltration the solvent was evaporated by evacuation at room temperature, the excess polymer was wiped from the specimen surface with paper tissue, and the weight gain of infiltrated samples was determined.

2.2. Warm pressing

A suspension of 20 g of the Taimicron TM DAR α-alumina powder in 40 ml of water-free cyclohexane and the amounts of the SP-M polymer equivalent to 3, 5, or 8 vol.% SiC (denoted below as CW3, CW5, and CW8) was vigorously stirred in a sealed glass flask under Ar for 2 h. The solvent was then evaporated by evacuation at room temperature. The polymer-coated powder was then passed through a 100 μm PE sieve, filled into a steel die with heating mantle, and uniaxially pressed at 50 MPa and 350 °C for 1 h to form cylindrical pellets of 6 mm height, and of 10 mm diameter.

2.3. Pressureless sintering

The specimens were placed in an alumina tube containing the protective powder bed of 50 wt.% Al_2O_3, 25 wt.% SiC and 25 wt.% C, and closed at both ends with graphite wool. The sintering was carried out in an electrical furnace with graphite heating elements in Ar, at temperatures between 1700 and 1850 °C, and with 3–5 h isothermal dwell at the maximum temperature. The sintered specimens were thoroughly cleaned from the residua of the powder bed, and the density was determined by Archimedes' method in water. The relative densities were obtained as the ratio of the Archimedes' densities, and the physical densities calculated by the rule of mixtures, using the physical density 3.986 g cm^{-3} for Al_2O_3 and 3.217 g cm^{-3} for SiC. The calculated values were then 3.963, 3.948, and 3.924 g cm^{-3} for the composites containing 3, 5, and 8 vol.% SiC, respectively. The specimens with the relative density of 90%, or higher, were then hot isostatically pressed for 2 h at 1700 °C, and at the 150 MPa pressure.

2.4. Characterisation

Polished and chemically etched (5 min in concentrated H_3PO_4 at 230 °C) cross sections of sintered specimens were examined by scanning electron microscopy (Zeiss, model EVO 40HV). The parameters of microstructure, i.e. the size distribution of alumina matrix grains, and of residual pores, the distribution and size of inter- and intragranular SiC particles,

were quantified by standard image analysis (Lucia, v. 4.82, LIM Praha, Czech Republic) of the micrographs. XRD measurements were carried out on a STOE STADIP powder diffractometer (STOE & CIE GmbH, Darmstadt, Germany) with Cu Kα radiation at the 2θ angle between 30 and 70°.

Hardness was measured by Vickers indentation of polished specimens at the maximum indentation load of 9.807 N. Indentation fracture toughness was determined from the length of radial cracks in the corners of residual imprints of Vickers indenter after 98.07 N loading. Fracture toughness was calculated from the length of radial cracks in the corners of residual plastic imprint by the method described by Anstis.[18] In all cases the length of radial cracks c was at least twice the length of diagonal of the residual plastic imprint, which is considered as the manifestation of well developed half-penny crack, and justifies the application of the Anstis' method.[18] However, it has to be emphasized that the measured values of indentation fracture toughness are not absolute, and they can serve, at the best, only for mutual comparison of qualitatively similar materials. The method has been selected due to its speed and convenience, and also due to the fact that a single small specimen is sufficient for the measurement. The reported values of hardness and fracture toughness were calculated as the mean values of at least 10 independent measurements.

3. Results and discussion

Fig. 1a and b show the temperature dependences of relative densities of sintered IP and CW specimens and their change after hot isostatic pressing. The CW specimens sintered at 1700 and 1750 °C, and those with 3 vol.% SiC were not used in HIP experiments, as their relative density was considered too low (in some case did not exceed 85%) to facilitate successful densification by HIP. However, in most cases HIP eliminated the residual porosity completely. The only exception were the specimens IPx_1700, where $x = 3$, 5, or 8, and represents the volume fraction of SiC in the material, and 1700 is the temperature of sintering. Despite the fact that these specimens were more than 90% dense, they still contained a significant amount of residual porosity after HIP. This ranged between 2.5 and 7.4 vol.%, for the specimens with 3, and 8 vol.% SiC, respectively. The result suggests that some open porosity was still present after sintering, which prevented densification during HIP. The residual porosity after HIP would then correspond to the volume fraction of open pores after sintering. As the residual porosity significantly influences the properties of composites, the samples IPx_1700, as well as the composites CW3 (all temperatures), CWx_1700 and CWx_1750 were excluded from indentation tests.

Hot isostatic pressing eliminated the porosity (to a fraction of volume per cent) in the materials, whose relative density after pressureless sintering was higher than 98%. In some cases the relative density even exceeded 100%, which is the consequence of partial decomposition of the specimen, and loss of SiC during HIP. As reported before,[15] loss of SiC at temperatures above 1700 °C was encountered during high-temperature densification of polymer-derived nanocomposites. Intimate contact between the grains of alumina powder and particles of SiC formed from

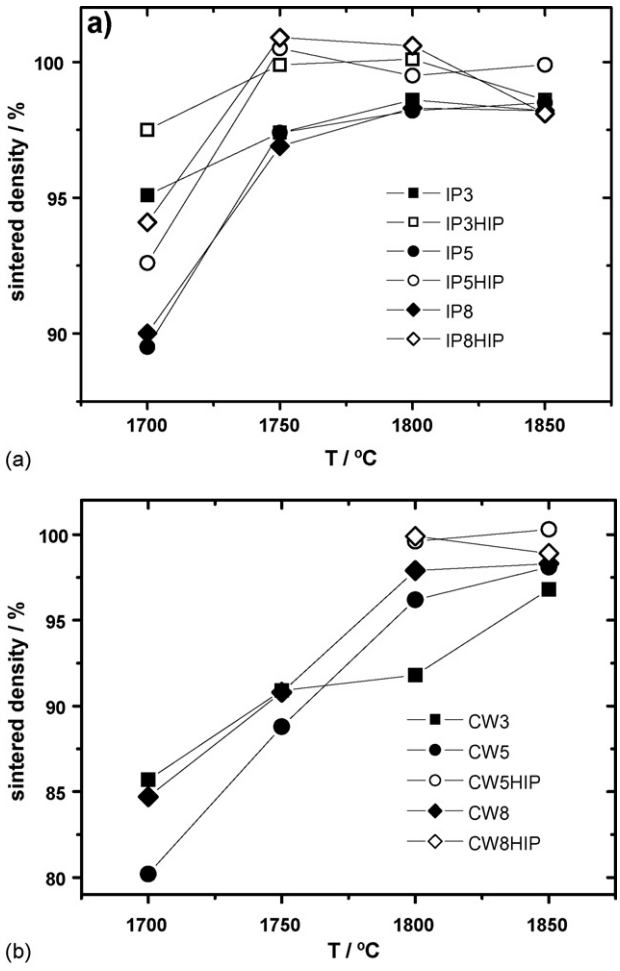

Fig. 1. Relative density of composites IP (a) and CW (b) after pressureless sintering and hot isostatic pressing.

a liquid precursor facilitates chemical reactions between the two substances, and suboxides of aluminium are formed, accompanied by development of CO, e.g:

$$Al_2O_3 + SiC \rightarrow Al_2O + SiO + CO \quad (1)$$

Decomposition in the course of pressureless sintering was suppressed by the use of a powder bed, which produces carbon monoxide and shifts the reaction equilibrium towards the reactants. In order to facilitate better action of gas pressure media the powder bed was not used during HIP: a weight loss was therefore observed in some cases. As the exact reaction sequence responsible for the weight loss is not known, and the evolution of a variety of gaseous species is possible according to the literature (SiO, CO, AlO, Al_2O, Al(g))[19,20] determination of the exact volume fraction of SiC in HIP-ed materials is not possible. The calculation of theoretical densities from the assumption of 3, 5, or 8 vol.% SiC in the material can then underestimate the real density of the composite.

Fig. 2a–d show the microstructures of the specimens CW8_1800 (a and b) and CW8_1850 (c and d) before, and after HIP. Table 1 summarises the results of image analysis, showing the mean sizes of alumina matrix grains, and of inter- and intragranular SiC inclusions before, and after HIP. Although not

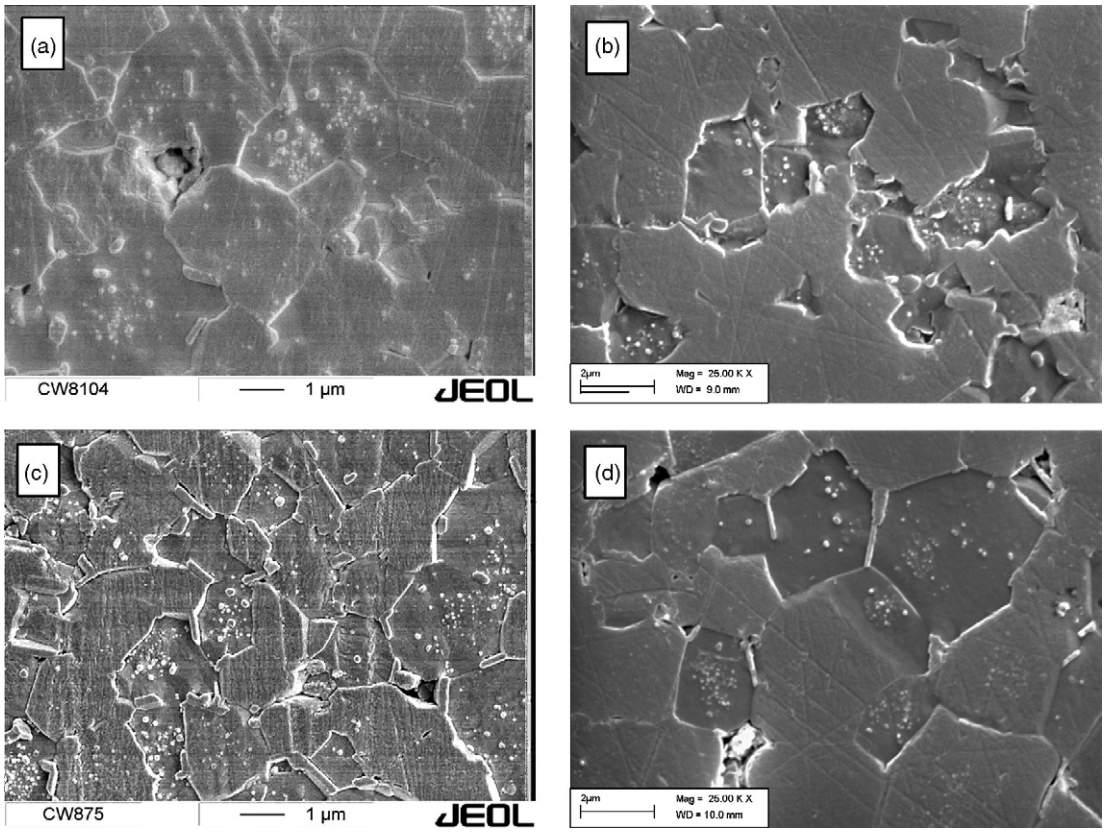

Fig. 2. Microstructures of CW specimens containing 8 vol.% of SiC after 5 h pressureless sintering at 1800 °C (a) followed by HIP (b), and of the specimens with the same composition sintered for 3 h at 1850 °C (c) followed by 2 h HIP at 1700 °C (d).

immediately obvious from the micrographs, the image analysis revealed that alumina matrix grains grew in the course of HIP. The grain size is expressed in terms of the equivalent circle diameter (i.e. the diameter of circle with the same area as the area of the measured grain). Grain growth was most pronounced in composites with 3 vol.% SiC, due to weaker pinning effect of smaller number of SiC particles. The mean sizes of SiC inclusions, both inter- and intragranular, also increased after HIP. According to Carroll et al., sufficient self-diffusion is present in SiC particles at the temperature of 1550 °C, to account for rounding of originally angular SiC particles.[7] Diffusion processes, which are responsible for growth of SiC particles, are therefore likely to occur at the temperature of HIP, i.e. at 1700 °C. However, the coarsening of SiC particles is mostly apparent. Growing alu-

Table 1
The mean sizes of alumina matrix grains, and of inter- and intragranular SiC inclusions in composites prepared by warm pressing (CW), after pressureless sintering (PS) and after PS followed by hot isostatic pressing (HIP)

Sintering	Specimen	ν(SiC) (vol.%)	CW					
			$D_{50}(Al_2O_3)$ (μm)		$D_{50}(SiC_{intra})$ (nm)		$D_{50}(SiC_{inter})$ (nm)	
			PS	HIP	PS	HIP	PS	HIP
1700 °C/5 h	CW3_1700	3	1.5	n.m.	125	n.m.	n.m.	n.m.
	CW5_1700	5	0.9	n.m.	86	n.m.	118	n.m.
	CW8_1700	8	n.m.	n.m.	70	n.m.	118	n.m.
1750 °C/5 h	CW3_1750	3	1.9	n.m.	123	n.m.	201	n.m.
	CW5_1750	5	1.0	n.m.	114	n.m.	207	n.m.
	CW8_1750	8	0.8	n.m.	96	n.m.	184	n.m.
1800 °C/5 h	CW3_1800	3	2.0	3.1	161	209	251	487
	CW5_1800	5	1.2	1.8	159	149	154	267
	CW8_1800	8	1.0	1.2	88	138	214	278
1850 °C/3 h	CW3_1850	3	n.m.	n.m.	n.m.	n.m.	n.m.	n.m.
	CW5_1850	5	1.5	2.0	88	166	143	407
	CW8_1850	8	1.2	1.0	89	91	186	249

mina grains engulf SiC particles, which were originally, after sintering, located at grain boundaries. These coarser, originally intergranular, particles then shift the mean size of intragranular SiC particles to higher values. The same applies for intergranular SiC inclusions: as smaller particles are engulfed by growing alumina grains, only very large particles stay at grain boundaries, and the mean is shifted to higher values.

Fig. 3a and b show the hardness of HIP-ed composites, and the relative change of hardness after HIP with respect to PS specimens. The highest hardness was measured in specimens containing 5 vol.% of SiC (Fig. 3a). The hardness of composites CW5 and IP5 ranged between 20.5 and 21.5 GPa, respectively. These values are not particularly high, but fall well into the interval usually reported for Al_2O_3–SiC composites with the same volume fraction of SiC.[12] The hardness of composites IP*x*_1850 is low after HIP (Fig. 3a), ranges between 18.5 and 19.5 GPa, and is somewhat lower than the hardness of PS composites of the same composition. The trend is thus reversed in comparison with PS specimens where hardness tended to increase with increasing temperature of sintering.[17] Fig. 3b shows the relative change of hardness after HIP, with respect to the PS specimens of the same composition. In the composites IP*x*_1750, and IP*x*_1800 the hardness increased by 1–10% after HIP. The increase can be most likely attributed to decrease of residual porosity. However, in IP*x*_1850 the hardness decreased with respect to the PS specimen, despite the fact that residual porosity was slightly lower, and no significant weight loss indicating decomposition of the sample could be measured (the weight loss in this batch of materials was usually less than 0.1%). However, the decrease did not exceed 6% and considering the scatter of measured values (standard deviation between 3 and 6% of the mean) its statistical significance is questionable. Fig. 4 shows a loose correlation between the Vickers hardness and the relative density of HIP-ed composites, irrespective of the content of SiC.

The problem of fracture toughness of Al_2O_3–SiC nanocomposites is rather complex, and there are many works published, which attempt to solve the question of the influence of volume fraction of SiC, the fraction and size of inter- and intragranular SiC inclusions, residual stresses, and other factors.[7,10–13,21,22] The only generally accepted fact seems to be the change of fracture mode from intergranular in monolithc alumina to mixed, or transgranular in nanocomposites, with corresponding increase of fracture energy. Levin et al. suggested that the toughening in particulate composites was the result of fine balance between matrix weakening and grain boundary strengthening by residual stresses around intragranular SiC particles. Their model implies that any increase of fracture toughness can be obtained only for small additions (less than 5 wt.%) of SiC. Maximum of 40% increase of toughness with respect to monolithic alumina can be expected according to this model.[22] The grain boundary strengthening effect of SiC nanoinclusions has been confirmed by measurement of grain boundary-interface dihedral angles in Al_2O_3/SiC by Jiao et al. who found that the interfacial fracture energy between SiC and alumina is more than twice the alumina grain boundary fracture energy.[21] Carroll et al., concluded that the fracture toughness of nanocomposites increase with the SiC particle size, but the increase is negligible with respect to the monolithic alumina. Moreover, according to the authors, any

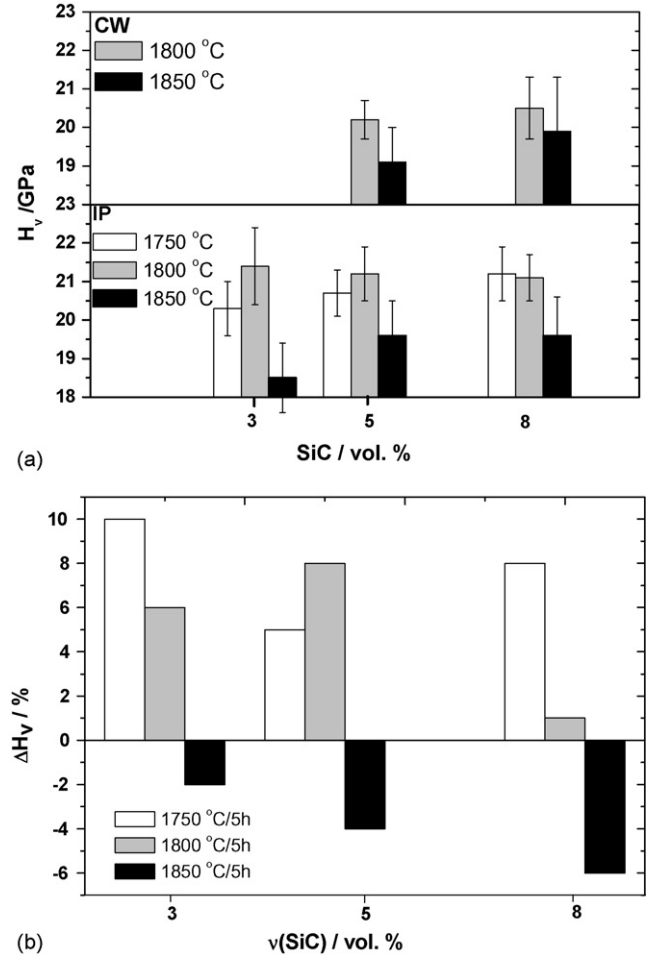

Fig. 3. Hardness of HIP-ed specimens (a) and relative change of hardness of HIP-ed specimens IP with respect to the hardness of PS composites of identical composition (b). The temperatures shown in the legend represent the temperatures of sintering preceding the HIP treatment.

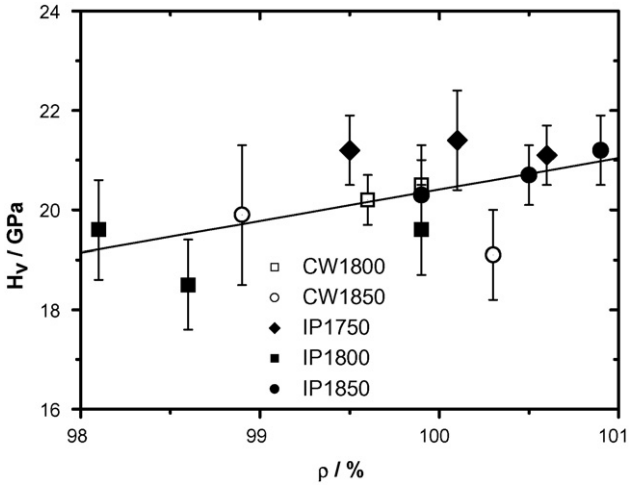

Fig. 4. Vickers hardness vs. relative density of the HIP-ed composites.

effect of SiC particle size is difficult to separate from effects of processing.[7] In the contrary, Xu et al. found no toughening effect of intragranular SiC particles, but they observed 15% toughening in a 12 vol.% SiC nanocomposite, which they attributed to SiC particle-attracted crack deflection and crack impediment by large (200–300 nm) intergranular SiC particles.[11] To add to the confusion, Perez-Rigueiro et al. observed that fracture toughness of alumina/silicon carbide nanocomposites measured through the single-edge V-notched beam technique was not significantly affected either by the fraction of nanoparticles, or their size.[12]

The polymer-derived nanocomposites studied in this work all exhibited a mixed mode of crack propagation, with significant amount of transgranular fracture. Detailed examination of the crack path revealed that the propagating crack meets SiC particles, either inter-, or intragranular, only occasionally. In most cases the propagation of crack was straightforward with few deviations from the direct path. Some instances are shown, and marked with Arabic numbers, in the Fig. 5. Number 1 (Fig. 5a) shows the instance when the crack was deflected from transgranular path by a large, elongated intergranular particle, which weakened the grain boundary. Number 6 (Fig. 5c) marks the place where the crack was deflected from its original direction within a large alumina grain by a large intragranular SiC inclusion. However, in most cases (No. 2, 3, 5), the crack crosses elongated intergranular SiC particles without any observable change of direction, SiC particles remain intact, and act as bridging ligaments, with possible toughening effect. Nevertheless, relatively rare occurrence of such events indicates that any toughening effect would be small.

One of the most interesting features was the strong influence of processing conditions on fracture resistance of the composites (Fig. 6a). In HIP-ed IP specimens the highest fracture toughness of $4.9 \pm 0.2\ \mathrm{MPa\,m^{1/2}}$ was measured in composites sintered at 1800 °C. This value was achieved for all samples sintered at this temperature, irrespective of the volume fraction of SiC. Sintering at 1850 °C, followed by HIP, resulted in lower fracture toughness, with maximum at 5 vol.% SiC ($4.3 \pm 0.2\ \mathrm{MPa\,m^{1/2}}$). Moreover, the fracture toughness of IP*x*_1850 decreased further after HIP by as much as 15% with respect to the FS composites of the same composition (Fig. 6b). No such effect was observed in the specimens sintered at lower temperatures, where any changes of fracture toughness after HIP ranged within margins of experimental error (0–6%). Such results were surprising, as the materials sintered at 1850 °C contained the highest fraction of elongated intergranular SiC grains, with strongest expected toughening effect. The reason for such behaviour is not clear, but the fact that the decrease of fracture toughness can be seen only in the IP specimens sintered at 1850 °C indicates that it can be related to the presence of phases formed at temperatures exceeding 1800 °C. Reports exist on formation of Al_4C_3, Al_2OC, and even of the eutectic melt of Al_4C_3–Al_2O_3 ($T_e = 1815$ °C) in Al_2O_3–SiC systems heat treated at temperatures exceeding 1800 °C.[19] However, if formed, the amount of these phases was too low to be detected by X-ray analysis. Apart of α-Al_2O_3 and β-SiC, only quartz in small amounts was identified from X-ray diffraction patterns. The presence of SiO_2 is an evidence of partial oxidation of the polymeric precursor and/or polymer-derived SiC in the course of preparation and together with possible formation of the eutectic melt Al_4C_3–Al_2O_3 represents a possibility of formation of glassy grain boundary phase. However, at this stage no evidence exists that any grain boundary glass is present in IP composites.

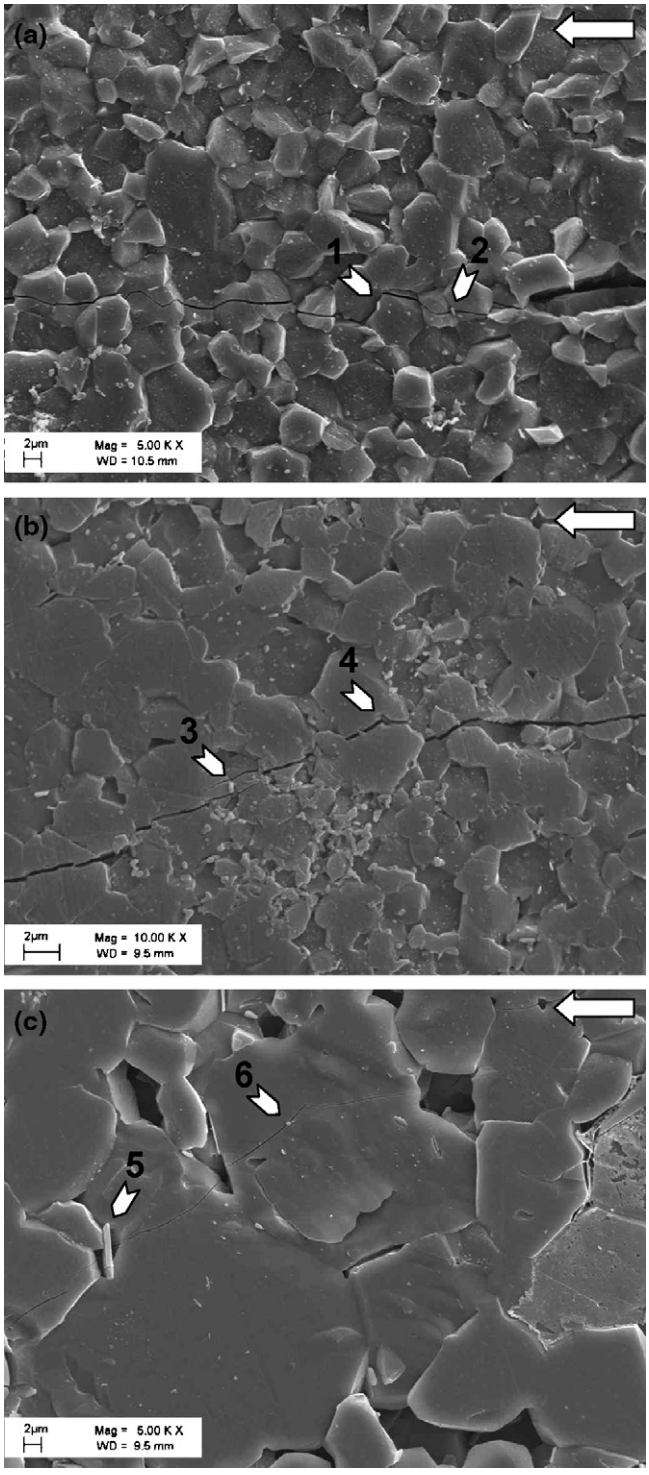

Fig. 5. Crack propagation in the composites IP5_1800 (a), IP8_1800 (b), and IP3_1850 (c). The white arrow in upper right hand corner indicates the direction of crack propagation.

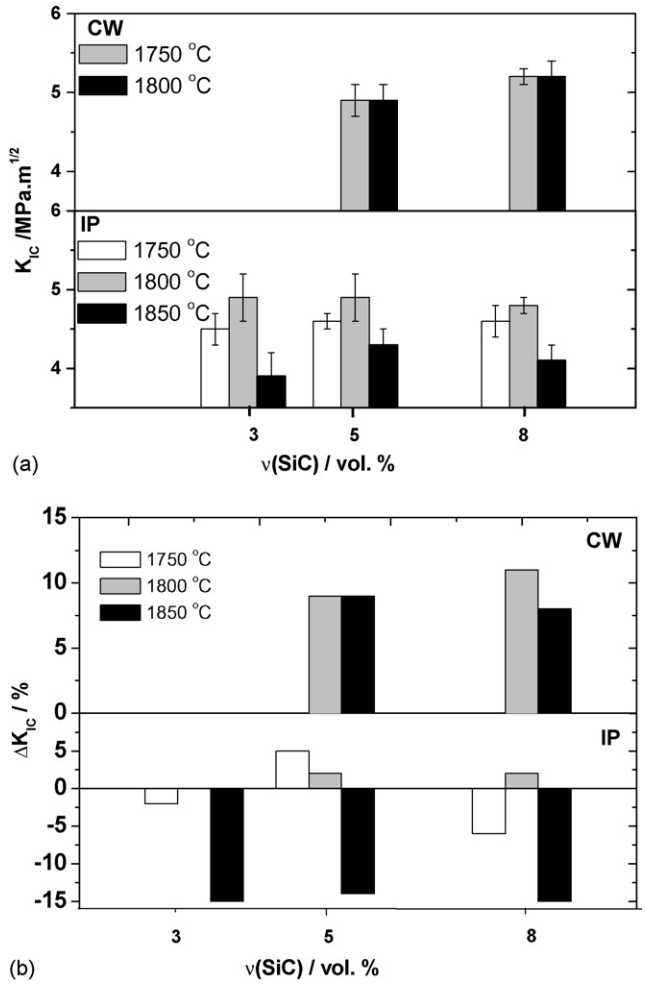

Fig. 6. Indentation fracture toughness of HIP-ed specimens (a) and relative change of fracture toughness of HIP-ed specimens with respect to the toughness of PS composites of identical composition (b).

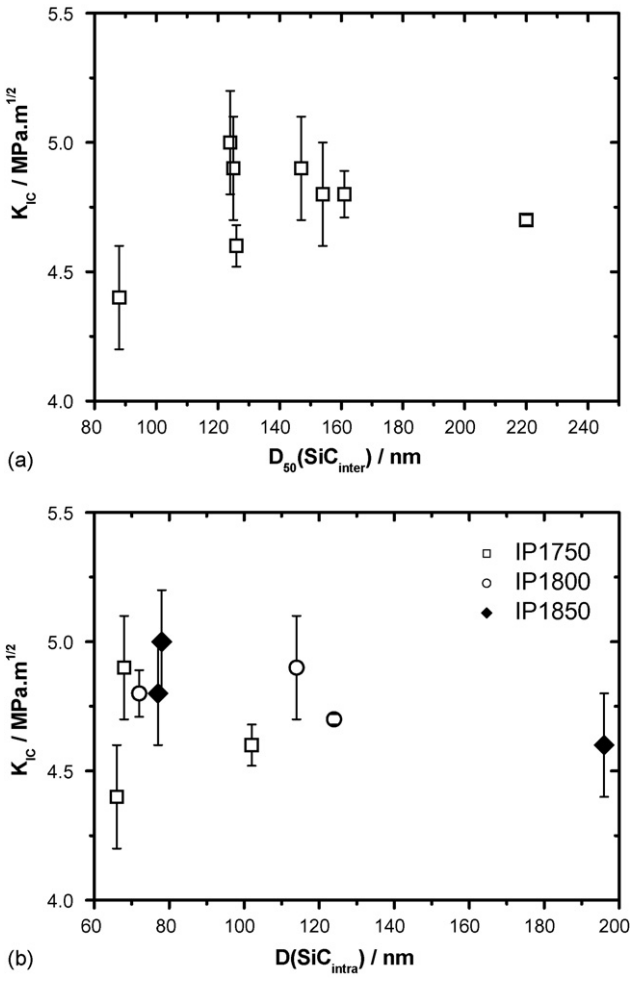

Fig. 7. The relation between the size of intergranular (a) and intragranular (b) SiC nanoinclusions and the fracture resistance of IP composites.

Due to large scatter of experimental data there was not possible to draw unambiguous conclusions on the influence of the size of intra- and intergranular SiC inclusions on fracture resistance of IP composites (Fig. 7a and b). The maximum of fracture toughness seems to be achieved in composites with fine-grained SiC, at around 80 nm size for intragranular, and at 120 nm for intergranular particles, and decreases with increasing size of SiC particles. Very fine intergranular (∼90 nm), and intragranular (∼60 nm) SiC seem to have no toughening effect, but definite conclusions could not be drawn from a single point.

The CW specimens behaved in a different way. The maximum toughness after sintering, 4.8 ± 0.1 MPa m$^{1/2}$, was measured in the composite CW8_1850. Generally, fracture resistance of CW materials (at least of those whose residual porosity was eliminated to the extent, which facilitated the measurement) increased with the temperature of sintering. All composites sintered at the same temperature had similar fracture toughness irrespective of the volume fraction of SiC. Hot isostatic pressing resulted in the net increase of K_{IC} of approximately 10% for all specimens measured (Fig. 6b), achieving the maximum of 5.2 ± 0.2 MPa m$^{1/2}$ in the composite CW8_1850 (Fig. 6a).

More detailed microstructure analysis revealed that the K_{IC} of both the FS and HIP composites prepared by warm pressing increased with increasing volume fraction of intergranular SiC particles (Fig. 8). This result is in accord with the work

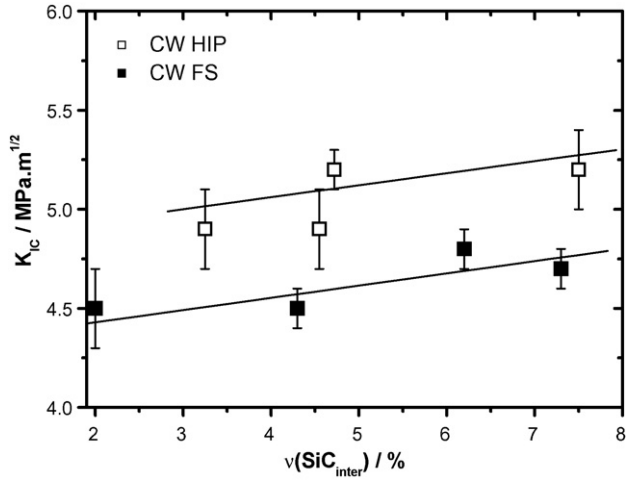

Fig. 8. The dependence of fracture toughness of CW composites before, and after HIP on the volume fraction of intergranular SiC particles.

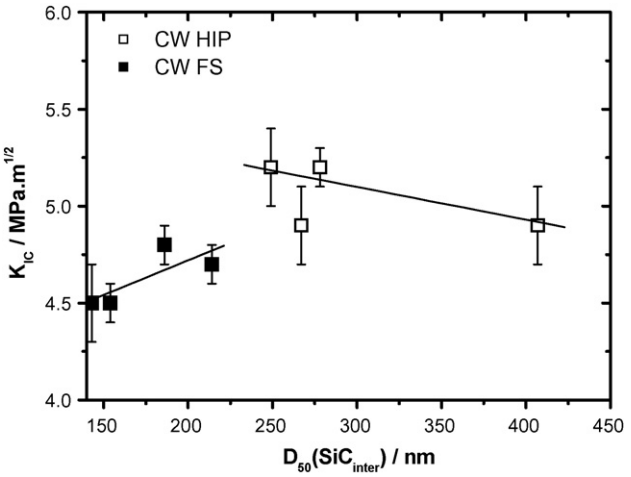

Fig. 9. The dependence of fracture toughness of CW composites before, and after HIP, on the mean size of intergranular SiC particles.

of Xu et al., who concluded that intergranular particles provide most of the toughening in Al_2O_3–SiC nanocomposites, mainly through a SiC particle-attracted crack deflection mechanism and crack impediment. The cracks are then more likely to propagate through matrix grain boundaries containing a higher than average density of intergranular SiC particles, which are weakened by residual tensile stresses around the SiC particle with lower than the surrounding matrix thermal expansion coefficient.[11] Interestingly, HIP shifted the K_{IC} values of all measured materials to higher values, so that the fracture toughness of the composite with the same volume fraction of intergranular inclusions tends to be higher after HIP. As shown above, HIP results in growth of both the alumina matrix grains and inter- and intragranular SiC particles. Although the growth of SiC particles by diffusion is possible, its contribution is supposed to be small and the coarsening is only apparent. Still larger SiC particles are entrapped in the course of HIP by growing alumina grains, which shifts the mean size of both inter- and intragranular SiC particles to higher values. The grain boundaries are then occupied by smaller amount of larger SiC inclusions, and their weakening effect is stronger. The crack is then more readily deflected along the grain boundary. The crack can also be deflected by the intergranular particle itself if the size of the particle is large enough.[11] However, the toughening effect of intergrain SiC inclusions would decrease as soon as their number is reduced by grain boundary motion to an extent when only few boundaries are weakened by their presence. Fig. 9 shows the fracture toughness of CW composites before, and after HIP, as a function of the mean size of intergranular SiC particles. At first, the K_{IC} clearly increases with the size of intergrain SiC, achieving maximum at about 250 nm. After that the HIP-induced growth of alumina matrix grains reduces the number of intergrain SiC particles to an extent when their toughening effect is diminished, and the K_{IC} decreases.

The results discussed above indicate that the fracture toughness of Al_2O_3/SiC nanocomposites is to certain extent influenced by the volume fraction and size of intergrain SiC inclusions, as confirmed by microstructure analysis of CW composites prepared by warm pressing, a polymer precursor-coated alumina powder. However, the toughening effect of intergranular SiC particles was not observed in the composites IP prepared by infiltration of a pre-sintered alumina matrix with the liquid precursor. The role of intragranular SiC inclusions is also questionable, as no clear correlation between their size and volume fraction, and the fracture toughness could be found. Hot isostatic pressing influences the fracture resistance of the composites IP and CW in a different way. While no significant change, or even 15% decrease of fracture toughness was measured in IP composites after HIP, the K_{IC} of CW composites increased by about 10%, irrespective of the volume fraction of SiC in the material. The reason of the observed decrease of fracture toughness after HIP in IP composites sintered at 1850 °C is not clear at present, but we suggest it is related to the presence of silica detected in the specimens by X-ray diffraction, together with possible formation of grain boundary glass with the composition of the eutectic melt Al_4C_3–Al_2O_3 with addition of SiO_2.

4. Conclusions

Hot isostatic pressing was applied as the means of elimination of residual porosity from polymer-derived composites Al_2O_3–SiC prepared by pressureless sintering. Although majority of specimens was successfully densified, and the residual porosity of HIP-ed specimens was always less than 1% (in comparison with 2–3%) for pressureless sintered materials, the influence on mechanical properties is ambiguous. Hardness increase of the specimens sintered at 1750 and 1800 °C was observed after HIP, but the change usually did not exceed 10%. Fracture toughness of the composites IP did not chance appreciably after HIP, and the observed increase, or decrease was mostly within the range of experimental error. The indentation fracture toughness of IP specimens sintered at 1850 °C was impaired by HIP, and up to 15% toughness decrease was measured. The fracture resistance of the CW composites increased after HIP by about 10%, irrespective of the volume fraction of SiC, and the temperature of sintering. The increase of toughness is attributed to toughening effect of intergrain SiC inclusions and is correlated with their size and volume fraction.

Acknowledgements

The financial support of this work by the Alexander von Humboldt Foundation, Bonn, Germany, by the grant number O051/03R80600/03R0603, and by the Slovak National Grant Agency VEGA, under the contract number 2/3101/23, is gratefully acknowledged.

References

1. Niihara, K., New design concept of structural ceramics–ceramic nanocomposites. *J. Ceram. Soc. Jpn.*, 1991, **99**, 974–982.
2. Stearns, L. C. and Harmer, M. P., Particle-inhibited grain growth in Al_2O_3–SiC: 1. Experimental results. *J. Am. Ceram. Soc.*, 1996, **79**, 3013–3019.
3. Sternitzke, M., Dupas, E., Twigg, P. C. and Derby, B., Surface mechanical properties of alumina matrix nanocomposites. *Acta Mater.*, 1997, **45**, 3963–3973.

4. Ohji, T., Jeong, Y.-K., Choa, Y.-H. and Niihara, K., Strengthening and toughening mechanisms of ceramic nanocomposites. *J. Am. Ceram. Soc.*, 1998, **81**, 1453–1460.
5. Chou, I. A., Chan, H. M. and Harmer, M. P., Machining-induced surface residual stress behavior in Al_2O_3–SiC nanocomposites. *J. Am. Ceram. Soc.*, 1996, **79**, 2403–2409.
6. Thompson, A. M., Chan, H. M. and Harmer, M. P., Crack healing and stress-relaxation in Al_2O_3–SiC nanocomposites. *J. Am. Ceram. Soc.*, 1995, **78**, 567–571.
7. Carroll, L., Sternitzke, M. and Derby, M., Silicon carbide particle size effects in alumina-based nanocomposites. *Acta Mater.*, 1996, **44**, 4543–4552.
8. Wu, H. Z., Lawrence, C. W., Roberts, S. G. and Derby, B., The strength of Al_2O_3/SiC nanocomposites after grinding and annealing. *Acta Mater.*, 1998, **46**, 3839–3848.
9. Zhao, J., Stearns, L. C., Harmer, M. P., Chan, H. M. and Miller, G. A., Mechanical behavior of alumina silicon-carbide nanocomposites. *J. Am. Ceram. Soc.*, 1993, **76**, 503–510.
10. Pezzotti, G. and Sakai, M., Effect of a silicon carbide "nano-dispersion" on the mechanical properties of silicon nitride. *J. Am. Ceram. Soc.*, 1994, **77**, 3039–3041.
11. Xu, Y., Zangvil, A. and Kerber, A., SiC nanoparticle-reinforced Al_2O_3 matrix composites: role of intra- and intergranular particles. *J. Eur. Ceram. Soc.*, 1997, **17**, 921–928.
12. Perez-Rigueiro, J., Pastor, J. Y., Llorca, J., Elices, M., Miranzo, P. and Moya, J. S., Revisiting the mechanical behavior of alumina silicon carbide nanocomposites. *Acta Mater.*, 1998, **46**, 5399–5411.
13. Jiao, S. and Jenkins, M. L., A quantitative analysis of crack-interface interactions in alumina-based nanocomposites. *Phil. Mag. A*, 1998, **78**, 507–522.
14. Galusek, D. and Riedel, R., Al_2O_3–SiC nanocomposites by infiltration of alumina matrix with a liquid polycarbosilane. In *Innovative processing and synthesis of ceramics, glasses and composites VIII, ceramic transactions*, *166*, ed. N. P. Bansal. American Ceramic Society, Columbus, USA, 2004, pp. 87–100.
15. Galusek, D., Riedel, R. and Balog, M., Polymer-derived Al_2O_3–SiC nanocomposites: preparation route vs. microstructure. *Key Eng. Mater.*, 2005, **290**, 121–128.
16. D. Galusek, E. Čierniková, R. Riedel, unpublished results.
17. Galusek, D., Sedláček, J. and Riedel, R., Microstructure and mechanical properties of polymer-derived Al_2O_3–SiC micro-nanocomposites. In *107th annual meeting and exposition of the American ceramic society*, 2005.
18. Anstis, G. R., Chantikul, P., Marshall, D. B. and Lawn, B. R., A critical evaluation of indentation techniques for measuring fracture toughness: I. direct crack measurements. *J. Am. Ceram. Soc.*, 1981, **64**, 533–538.
19. Misra, A., Thermochemical analysis of the silicon carbide-alumina reaction with reference to liquid phase sintering of silicon carbide. *J. Am. Ceram. Soc.*, 1991, **74**, 345–351.
20. Baud, S., Thévenot, F., Pisch, A. and Chatillon, C., High temperature sintering of SiC with oxide additives: I. analysis in the SiC–Al_2O_3 and SiC–Al_2O_3–Y_2O_3. *J. Eur. Ceram. Soc.*, 2003, **23**, 1–8.
21. Jiao, S., Jenkins, M. L. and Davidge, R. W., Interfacial fracture energy-mechanical behaviour relationship in Al_2O_3/SiC and Al_2O_3/TiN nanocomposites. *Acta Mater.*, 1997, **45**, 149–156.
22. Levin, I., Kaplan, W. D., Brandon, D. G. and Layyous, A. A., Effect of SiC submicrometer particle size and content on fracture toughness of alumina–SiC "nanocomposites". *J. Am. Ceram. Soc.*, 1995, **78**, 254–256.